PERFORMANCE ASSESSMENT OF SHELL AND TUBE HEAT EXCHANGER BASED SUBCRITICAL AND SUPERCRITICAL ORGANIC RANKINE CYCLES

by

Anil ERDOGAN[a*] and C. Ozgur COLPAN[a,b]

[a] The Graduate School of Natural and Applied Sciences, Dokuz Eylul University, Izmir, Turkey
[b] Department of Mechanical Engineering, Faculty of Engineering, Dokuz Eylul University, Izmir, Turkey

Original scientific paper
https://doi.org/10.2298/TSCI171101019E

In this study, thermal models for subcritical and supercritical geothermal powered organic Rankine cycles are developed to compare the performance of these cycle configurations. Both of these models consist of a detailed model for the shell and tube heat exchanger integrating the geothermal and organic Rankine cycles sides and basic thermodynamic models for the rest of the components of the cycle. In the modeling of the heat exchanger, this component was divided into several zones and the outlet conditions of each zone were found applying logarithmic mean temperature difference method. Different Nusselt correlations according to the relevant phase (single, two-phase, and supercritical) were also included in this model. Using the system-level model, the effect of the source temperature on the performances of the heat exchanger and the organic Rankine cycle was assessed. These performance parameters are heat transfer surface area and pressure drop of tube side fluid for the heat exchanger, and electrical and exergetic efficiencies of the integrated organic Rankine cycles system. It was found that 44.12% more net power is generated when the supercritical organic Rankine cycle is used compared to subcritical organic Rankine cycle.

Key words: *shell and tube heat exchanger, subcritical, supercritical, organic Rankine cycle, geothermal, performance assessment, zone modeling*

Introduction

Fossil fuels have started to be replaced with renewable energy resources such as wind, solar, biomass, hydro, and geothermal in the power generating systems as the consumption of the fossil fuels and the concerns on the environmental problems (*e. g*. air pollution, global warming, and ozone depletion) have increased [1, 2]. In the locations where geothermal resources are available, geothermal power plants have been built since early 1960s; and the installation of these plants have increased significantly in the last decades [3-7]. These plants are based on organic Rankine cycle (ORC) technology, which can convert low-grade heat source into electrical energy [8, 9]. Although this technology is not new, researchers still work on the development of this cycle to increase the cycle efficiency and electricity generation. In order to obtain a high performance from this cycle, selection of the design (*e. g*. type of heat exchanger

* Corresponding author, e-mail: anilerdogan1992@hotmail.com

and turbine) and operating parameters (*e. g*. type of working fluid, source temperature, and turbine inlet temperature and pressure) plays a crucial role [10].

According to the temperature and pressure of the turbine inlet of an ORC, the cycle could operate either in subcritical or supercritical conditions. There are some studies on the devel-opment of subcritical ORC and their components through modeling and experimental studies. For example, Heberle and Bruggeman [11] studied the concepts of serial and parallel circuits of ORC. The selection of the fluid type was assessed for some operating parameters such as geothermal water inlet temperature and supply temperature of the heating system. The results of this study showed that for the serial case of ORC, isobutane is the most suitable working fluid type; whereas for the parallel case, isobutane and R227ea are the favourable working fluid types. Tempesti and Fiaschi [12] conducted a thermo-economic analysis of a micro-ORC system integrated with solar collectors. The thermo-economic performance of three different working fluids (*e. g*. R134a, R236fa, and R245fa) was compared. This analysis showed that R245fa is the most convenient fluid as it ensured the lowest price for electricity production and overall cost of the plant. Wang *et al*. [13] developed a mathematical model for subcritical ORC and conducted a parametric optimization using simulated annealing method. The results of their study showed that R123 is the best choice for the temperature range 100-180°C; whereas R141b is the suitable fluid for the temperature higher than 180 °C. Marion *et al*. [14] proposed a mathematical model for subcritical ORC integrated with the solar-thermal collector. R134a, R227ea, and R365mfc were considered as the different working fluid types. Their results showed that higher performance is obtained when R365mfc is used as the working fluid; and the performances of ORC using R134a and R227ea follow it, respectively. Kosmadakis *et al*. [15] presented a detailed experimental investigation of a small-scale subcritical ORC having the working fluid as R404A. In addition, ORC system is coupled with PV/T collectors and performance assessment was conducted comparatively. The experimental tests were conducted at laboratory conditions for summer and winter seasons. The most important result of laboratory tests is that ORC system can achieve sufficient thermal efficiency when working at very low temperature. Barbazza *et al*. [16] modeled a solar driven small scale ORC with turbogenerator. They also conducted an optimization study using genetic algorithm method. In this optimization study, evaporating pressure, minimum allowable temperature difference of the evaporator, and condenser and ORC working fluids (R1234yf, R1234ze, R245fa, R245ca, and n-pentane) were selected as decision variables; whereas the net power output, and the system volume were selected as objective functions. The results of this study showed that the minimum allowable temperature difference of the evaporator and condenser had significant effect on the performance of the system. In addition, R1234yf and R1234ze were the most appropriate working fluids to increase the performance of the system.

A supercritical ORC generally yields higher power output compared to a subcritical cycle; however higher investment cost, and selecting appropriate materials for the components such as turbine, heat exchanger, and fasteners such as vanes are the main disadvantages of the supercritical cycle [17]. There are some studies on the design and modelling of supercritical ORC systems and their components. For example, Wang *et al*. [18] proposed a regenerative supercritical and subcritical dual loop ORC system. A mathematical model was employed to analyze the performance of the system (the cycle efficiency and the net power output). In addition, they presented the effects of regeneration and operating parameters such as turbine inlet pressure and temperature on the performance of the subcritical and supercritical ORC dual loop. The results of this study showed that dual loop ORC system achieved

higher performance than the traditional ORC systems. Dong *et al*. [19] presented the selection of the working fluid type and determination of cycle parameters through a thermodynamic modeling study. They found that Siloxane MM is the most appropriate working fluid for high temperature ORC system (higher than 200 °C). Turbine inlet temperature is found to be more influential than the inlet pressure of the turbine on the ORC efficiency. Hsieh *et al*. [20] experimentally examined a 20 kW supercritical ORC having a screw turbine and R218 as the working fluid in order to investigate the system performance at the heat source temperature of 90-100 °C in both subcritical and supercritical conditions. The results of this study showed that the thermal efficiency of the supercritical ORC was 5.7%, 5.38%, and 5.28% for the heat source temperature of 90 °C, 95°C, and 100°C, respectively. Shengjun *et al.* [21] conducted a thermodynamic and economic performance study for both subcritical and supercritical geothermal powered ORC systems for low temperature geothermal resource temperature levels (*i. e*. 80-100 °C). They found that R123 as the working fluid type yields the highest performance in subcritical ORC; whereas R125 as the working fluid type provides favorable economic and environmental performance in supercritical ORC cycle. Vetter *et al*. [22] conducted a thermodynamic analysis of an ORC utilizing the energy of low temperature geothermal wells. They discussed the effect of the geothermal brine inlet temperature on the performance of both subcritical and supercritical ORC. They found that using propane instead of CO_2 yields higher performance of the cycle compared.

Heat exchangers are critical elements affecting the performance and cost of ORC [23]. They can be classified according to construction type such as shell and tube, plate, compact, and finned tube. Shell and tube heat exchangers have been preferred for large-scale ORC applications since they can be used at higher operating temperature and pressure, and also tube leaks around the heat exchangers are easily identified [24]. For small-scale ORC applications, plate type heat exchanger has been used since they can be used at lower mass flow rates, pressures and temperatures, and they have lower manufacturing and maintenance costs [25]. There are some studies in the literature on the design and modelling of heat exchangers for ORC applications. For example, Erdogan *et al*. [26] developed a detailed thermal model for the shell and tube heat exchanger, which combines a PTSC and an ORC. Parametric studies were conducted to find the effect of some of the key design and operating parameters (*e. g*. inner tube diameter, baffle spacing, number of tubes, tube length, shell side and tube side working fluids) on the performance of the heat exchanger such as heat transfer surface area, and the pumping power. In addition, a optimization study using two-stage Taguchi method was applied to find the optimum design parameters that yield the minimum heat exchanger surface area and pumping power. The results of this study showed that the baffle spacing is the most dominant design parameter affecting the performance of the heat exchanger; and Therminol VP1 or Dowtherm A as the PTSC side fluid and R245fa or R600 as the ORC side fluid should be preferred. Zhang *et al*. [27] used three different heat exchangers which are plate heat exchanger, shell and tube heat exchanger, and finned tube heat exchanger in the ORC system to investigate the ORC cycle performance comparatively. They obtained the optimal evaporating pressure, pinch point temperature difference, net power output, and dynamic payback period corresponding to the minimum electricity cost. The results showed that the electricity production cost of both plate heat exchanger based evaporator and condenser is the highest. Lazova *et al*. [28] designed a supercritical helical coil heat exchanger and tested it under real operational conditions. Three heat transfer correlations, which were taken from the literature, were used for different working fluid types. The results showed the uncertainty of these correlations is approximately 20% for different operating conditions of an ORC.

Literature survey conducted shows that there are many studies on the thermodynamic analysis of ORC systems; however inclusion of detailed analysis of ORC components, especially heat exchangers, in the ORC system-level models is limited. In this study, a thermal model of a geothermal powered ORC, which includes zone-modeling approach for the shell and tube heat exchanger and simple thermodynamic models for the remaining components, is developed to compare subcritical and supercritical configurations. Using this model, the effect of source temperature on the design and performance of the shell and tube heat exchanger (the tube side pressure drop, the heat transfer surface area, and the exergetic efficiency and effectivevess of the heat exchanger) and the performance of the ORC system (the electrical and exergetic efficiencies) is investigated for both configurations.

System description

The process flow diagram of subcritical and supercritical geothermal powered ORC systems modeled in this study is shown in fig. 1. The operating principle of the ORC system is as follows. The geothermal brine extracted from production well enters the shell side of the heat exchanger (the shell and tubes are made of stainless steel). Here, it transfers its heat to the ORC working fluid. On the other hand, working fluid of the ORC system enters from the tube side of the heat exchanger. Depending on the cycle configuration, the working fluid exiting the tube side of the heat exchanger is at either subcritical or supercritical state. Then, the working fluid enters the turbine where the power is produced. After it leaves the turbine, it enters the following components consecutively before entering the heat exchanger again: the desuperheater, the air cooled condenser (ACC), the pump, and the desuperheater. On the other side, the geothermal brine exiting the heat exchanger is sent back to reinjection well.

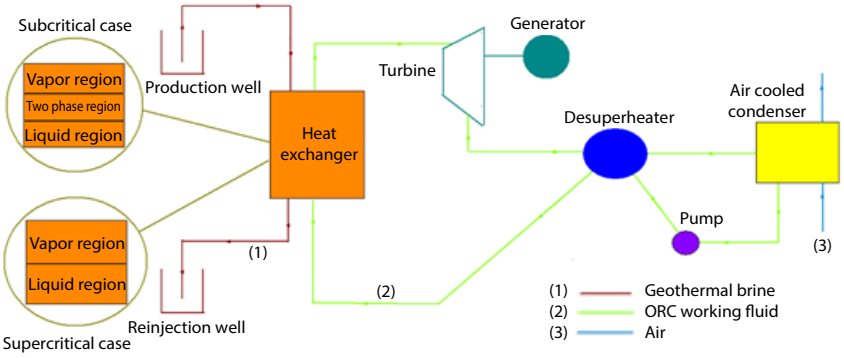

Figure 1. The schematic of the geothermal powered ORC system

Method

In this study, a detailed thermal model is used for the shell and tube heat exchanger for subcritical and supercritical ORC configurations; whereas energy balances are applied for the remaining ORC components. The modelling approach and the equations are given in the following subsections. These equations are solved using the engineering equation solver (EES) software. The main assumptions are given as follows.

- Heat losses from the components are neglected.
- Changes in kinetic and potential energies and their effects are ignored.
- The ORC system runs at steady-state conditions.
- The geothermal fluid leaving the production well is at saturated liquid state.

– In the two-phase zone of the subcritical ORC, the quality of ORC working fluid is taken as 0.5 in finding the thermophysical properties, the heat transfer coefficient, and the tube side pressure drop.
– Pressure drops in the desuperheater and the ACC are neglected.
– The thermophysical properties of cold (ORC working fluid) and hot (geothermal brine) fluids are calculated based on the average temperature of each zone.

Thermal model of the heat exchanger

In this subsection, the modelling equations and approach for the shell and tube heat exchanger are given. In this model, the heat exchanger is divided into three zones (liquid, two phase, and vapor) for subcritical ORC; whereas it is divided into two zones (liquid and vapor) for supercritical ORC. Zone-modeling approach is applied since the Nusselt number and pressure drop correlations change for each zone and a better estimation of thermophysical properties can be done using this approach. In the modelling of the heat exchanger, the temperatures of ORC working fluid entering and leaving each zone of heat exchanger in subcritical and supercritical ORC are considered to be known. Hence, the unknown temperatures of geothermal fluid entering and leaving the heat exchanger are found applying the energy balance for each zone. This model gives us the heat exchanger design (the heat transfer surface area) and performance parameters (the tube side pressure drop, the exergetic efficiency of the heat exchanger and the heat exchanger effectiveness).

In the modeling of the heat exchanger, the heat transfer rate between hot (geothermal brine) and cold (ORC working fluid) streams is first found applying an energy balance around the cold stream in a relevant zone. Then, the enthalpy of hot fluid outlet for each zone can be found applying energy balance around the hot stream in that zone.

Overall heat transfer coefficient (U) can be found using eq. (1):

$$\frac{1}{U}=\frac{D_o}{D_i}\frac{1}{h_i}+\frac{\ln\left(D_o/D_i\right)}{2\pi kL}+\frac{1}{h_o}+\frac{D_o}{D_i}R''_{fi}+R''_{fo} \tag{1}$$

where R''_{fi} and R''_{fo} are tube side and shell side fouling factors, which depends on fluid type, respectively. This parameter can be found in [24, 29]. To calculate the heat transfer coefficient of the tube side fluid (h_i), Reynolds number should be calculated first [24]. After calculating the Reynolds number, Nusselt number can be found according to the relevant phase and regime (laminar or turbulent). For single phase flow, two phase flow and supercritical phase, the relations given by Incropera *et al*. [30], Kandlikar [31] and Fang *et al*. [32] are used, respectively. Shell side heat transfer coefficient (h_o) is calculated using the equation proposed by McAdams [24].

Logarithmic mean temperature difference (LMTD) method is used to find the length of each zone. For this purpose, an iterative solution method is applied making an initial guess for the length of each zone. Using this initial guess, the equations given, eqs. (1) and (2), and data

Table 1. The input parameters of the heat exchanger model [26]

Parameters	Values
Shell side fluid	Geothermal water
Tube (ORC) side fluid	R134a
Number of pass	1
Number of tubes	1000
Inner diameter of tube [m]	0.016
Baffle spacing [m]	0.5
Tube pitch [m]	0.0254
Mass flow rate of shell side fluid [kgs^{-1}]	120.7
Mass flow rate of tube side fluid [kgs^{-1}]	213.4
Thermal conductivity of tube [Wm^{-1}K^{-1}]	63.9

given in tab. 1 are solved to calculate the overall heat transfer coefficient (U) for each zone. Using this value, eq. (2) is solved to calculate the length of each zone again. The iteration must continue until the absolute value of the difference between the initial guess of the length of the zone and the length of the zone found from eq. (2) is smaller than 10^{-3} m. It should be noted that there are separate iterations for each zones in this solution approach.

$$L_{zone} = \frac{\dot{Q}_{hx}}{UF\left[\frac{\left(T_{h,i}-T_{c,o}\right)-\left(T_{h,o}-T_{c,i}\right)}{\ln\frac{\left(T_{h,i}-T_{c,o}\right)}{\left(T_{h,o}-T_{c,i}\right)}}\right]\pi D_o N_T n_{\text{pass}}} \tag{2}$$

After finding the length of each zone using iterative solutions, the heat transfer surface area of the heat exchanger is calculated using eq. (3):

$$A_{\text{hx}} = \pi D_o L_{\text{hx}} N_T n_{\text{pass}} \tag{3}$$

The pressure drop of tube side between the inlet and exit streams is calculated for each zone. For single phase, two-phase and supercritical regions, pressure drop in tube side is given in eqs. (4)-(6), respectively. In these equations, f_{tp} and f_s denote the two phase and supercritical pressure friction factor and are given in [31] and [32], respectively.

$$\Delta P_{\text{tube}} = 4\exp\left[0.576-0.19\ln\left(\text{Re}_{\text{o}}\right)\right]L_{\text{zone}}\frac{n_{\text{pass}}}{D_i}+4n_{\text{pass}}\frac{\rho V^2}{2}\ (\text{single phase}[24]) \tag{4}$$

$$\Delta P_{\text{tube}} = \frac{2f_{tp}\dfrac{\dot{m}}{A}L_{\text{zone}}v_f}{D_i}\left[1+\frac{x\left(v_{\text{g}}-v_f\right)}{2v_f}\right](\text{two-phase [33]}) \tag{5}$$

$$\Delta P_{\text{tube}} = \frac{2f_s\dfrac{\dot{m}}{A}L_{\text{zone}}}{2\rho D_{\text{i}}}(\text{supercritical phase [32]}) \tag{6}$$

The heat exchanger effectiveness can be found using eq. (7):

$$\varepsilon_{\text{hx}} = \frac{\dot{Q}_{\text{hx}}}{\dot{m}_c\left(h_{h,i}-h_{c,i}\right)} = \frac{\dot{m}_h\left(h_{h,i}-h_{h,o}\right)}{\dot{m}_c\left(h_{h,i}-h_{c,i}\right)} \tag{7}$$

The exergetic efficiency of the heat exchanger can be found using eq. (8):

$$\eta_{\text{hx}} = \frac{\dot{m}_c\left[\left(h_{c,i}-h_{c,o}\right)-T_o\left(s_{c,i}-s_{c,o}\right)\right]}{\dot{m}_h\left[\left(h_{h,i}-h_{h,o}\right)-T_o\left(s_{h,i}-s_{h,o}\right)\right]} \tag{8}$$

Thermal model of the ORC systems

For the control volumes enclosing each component of the system, steady state mass and energy balances are applied using eqs. (9) and (10), respectively. Using these equations, the thermodynamic properties of each state, power produced by the turbine, power consumed by the pump, and net power output of the system can be found:

$$0 = \sum_i \dot{m}_i - \sum_e \dot{m}_e \tag{9}$$

$$0 = \sum_i \dot{m}_i \left(h_i + \frac{1}{2}V_i^2 + \mathrm{g}z_i\right) - \sum_e \dot{m}_e \left(h_e + \frac{1}{2}V_e^2 + \mathrm{g}z_e\right) + \dot{Q}_{cv} - \dot{W}_{cv} \tag{10}$$

The performance assessment parameters, which are electrical and exergetic efficiencies are calculated as given in eqs. (11) and (12), respectively:

$$\eta_{el} = \frac{\dot{W}_{\text{net}}}{\dot{Q}_{hx}} = \frac{\dot{W}_{\text{net}}}{\dot{m}_h \left(h_{h,i} - h_{h,o}\right)} \tag{11}$$

$$\eta_{ex} = \frac{\dot{W}_{\text{net}}}{\dot{E}_{h,i} - \dot{E}_{h,o}} = \frac{\dot{W}_{\text{net}}}{\dot{m}_h \left[\left(h_{h,i} - h_{h,o}\right) - T_o \left(s_{h,i} - s_{h,o}\right)\right]} \tag{12}$$

Results and discussion

In this section, the results and discussion on the effect of source temperature on the heat exchanger performance parameters (pressure drop of the tube side fluid of each zone, the heat transfer surface area, the heat exchanger effectiveness, the exergetic efficiency of the heat exchanger) and the overall ORC performance parameters (the electrical and exergetic efficiencies) are presented. One shell and one tube pass type heat exchanger is selected in the subcritical and supercritical ORC systems. The input parameters for the heat exchanger and ORC models are given in tabs. 1 and 2, respectively.

The results on the effect of source temperature on the design and performance of the heat exchanger for subcritical and supercritical ORC systems are presented in figs. 2(a) and 2(b). These figures also include a comparison between two different heat exchanger modeling approaches (single-zone and multi-zone). In single-zone modeling, the heat exchanger is considered as a whole and single-phase flow correlations are applied; whereas in multi-zone modeling, the equations given in the section *Method* are applied. Figures 2(a) and 2(b) show the change of heat transfer surface area and the tube side pressure drop for different source temperature, and subcritical and supercritical ORC. For the source temperature of 430 K, it was obtained that the heat transfer surface areas and the tube side pressure drops for both subcriticial and supercritical ORC obtained from single zone modelling approach are 744.5 m^2 and 835.6 m^2 and 341.6 kPa and 441.1 kPa, respectively; whereas the heat transfer surface area and the tube side pressure drops for both subcritical and supercritical ORC obtained from multi-zone modelling approach are calculated as 1173.07 m^2 and 844.7 m^2 and 987 kPa and 215.3 kPa, respectively. The multi-zone modelling approach is expected to give more accurate results since the thermo-pysical properties and heat transfer and pressure drop correlations were evaluated in a more precise way. Figure 2(a) shows that as the source temperature increases

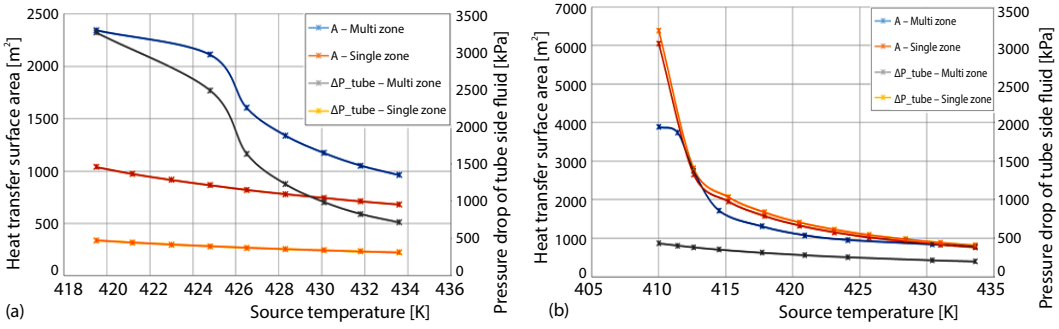

Figure 2. The effect of the source temperature on the heat transfer surface area and pressure drop of tube side fluid for R134a; (a) in subcritical ORC and (b) supercritical ORC

from 419.5 K to 433.6 K, the heat transfer surface area obtained from single zone modelling approach decreases (1039-681.4 m^2). This finding is mainly due to the fact that as the source temperature increases, the overall heat transfer coefficient given in eq. (1) increases from 955-990 W/m^2K. Since the area of the heat exchanger is inversely proportional to overall heat transfer coefficient, length of the heat exchanger decreases. The heat transfer surface area obtained from multi-zone modelling approach also decreases (2345.9-962.31 m^2) with an increase in the source temperature. Similar to the single-zone approach, length of each zone decreases when the source temperature increases. On the other hand, the change of the tube side pressure drop with respect to source temperature is also shown in fig. 2(a). As the source temperature increases, the tube side pressure drop obtained from single zone modelling approach decreases. This finding is mainly due to the decrease in the heat exchanger length. In addition, when the source temperature increases, the tube side pressure drop obtained from multi-zone modelling approach also decreases. This result can be clarified as follows. As the source temperature increases, the length of each zone decreases. In addition, in the two phase zone, the specific volume difference between the saturated vapor and saturated liquid states decreases. Due to this reason, the nominator of eq. (5) decreases, thus the tube side pressure drop in the two-phase zone decreases. For the supercritical ORC system, the effect of source temperature on the heat transfer surface area of the heat exchanger and tube side pressure drop is similar to that for the subcritical ORC. In the multi-zone modeling approach, the decrease in the tube side pressure drop with an increase in the source temperature can be explained as follows. As the source temperature increases, the viscosity and density of the ORC working fluid entering the vapor zone at wall temperature decrease. Thus, the supercritical pressure friction factor decreases. It was also found that the liquid zone pressure drop is higher than the vapor zone pressure drop for a given source temperature.

Table 2. Input parameters of the subcritical and supercritical ORC [2,26]

Common parameters	
The mass flow rate of air in the ACC [kgs^{-1}]	3240 [2]
The fan power in the ACC [kW]	600 [2]
The generator efficiency	98% [2]
The isentropic efficiency of the turbine	80% [2]
The pressure of the condenser [kPa]	947 [2]
The pressure of geothermal water entering the heat exchanger [kPa]	624.8 [2]
The temperature of geothermal water entering the heat exchanger [K]	433.6 [2]
Subcritical ORC parameters	
The pressure of ORC working fluid entering the heat exchanger [kPa]	3000 [26]
The temperature of ORC working fluid entering the heat exchanger [K]	343 [26]
The temperature of ORC working fluid entering the turbine [K]	370 [26]
Supercritical ORC parameters	
The pressure of ORC working fluid entering the liquid region zone of the heat exchanger [kPa]	4370 [2]
The temperature of ORC working fluid entering the liquid region zone of the heat exchanger [K]	360 [2]
The temperature of ORC working fluid leaving the supercritical region zone of the heat exchanger [K]	390 [2]

Figures 3(a) and 3(b) show the change of exergetic efficiency of the heat exchanger and the heat exchanger effectiveness on the subcritical and supercritical ORC, respectively. For the source temperature of 430 K, it was found that the exergetic efficiency of the heat exchanger for supercritical ORC (74.8%) is higher than that for the subcritical ORC (35.24%). However, the effectiveness of the heat exchanger for subcritical ORC (29.1%) is found to be higher than that of the supercritical ORC (24.94%). These figures show that when the source temperature increases from 417.7-433.6 K, the heat exchanger effectiveness for subcritical and supercritical ORC decreases from 32.6-28.2%, and 32.16-24.15%, respectively. These findings can be explained as follows. As the source temperature increases, the enthalpy of geothermal water entering the heat exchanger increase, thus the effectiveness of heat exchanger decreases. For the same range of increase in the source temperature, the exergetic efficiency for subcritical and supercritical ORC decreases from 41.25-18.02% and 80.27-72.42%, respectively. This trend is mainly due to the fact that when the source temperature increases, the entropy change between the inlet and exit streams of geothermal water decreases. This decrease increases the flow exergy change of the geothermal stream and the exergetic efficiency of heat exchanger decreases.

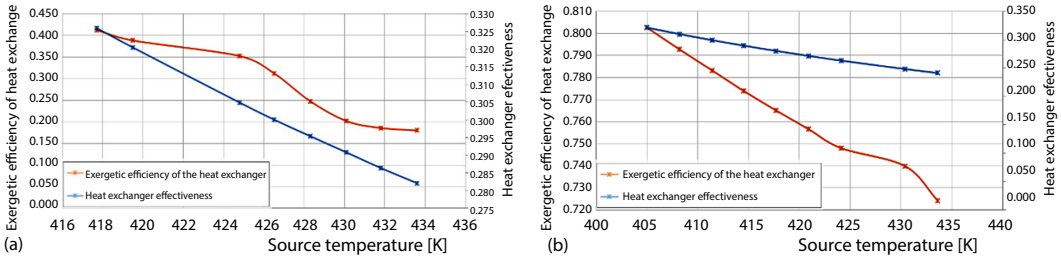

Figure 3. The effect of the source temperature on the exergetic efficiency of the heat exchanger and the heat exchanger effectiveness for (a) subcritical and (b) supercritical ORC

The effect of source temperature on the electrical and exergetic efficiencies of the subcritical and supercritical ORC is also assessed. When the source temperature increases from 405-433.6 K, the electrical efficiency of the subcritical and supercritical ORC are constant and are calculated as 7.85% and 15%, respectively. This trend is due to the fact that, the enthalpy change between the inlet and exit streams of the cold fluid (*i. e*. ORC working fluid) does not change due to the considered inlet parameters of the model. On the other hand, the exergetic efficiency of the subcritical and supercritical ORC decrease from 30.52-10.3% and 60.7-52.19%, respectively, with the same increase in the source temperature. This trend is mainly due to the fact that, as the source temperature increases, the flow exergy rate change increases since the entropy change between the inlet and exit streams of geothermal fluid for each zone decreases.

Conclusions

In this study, thermodynamic models for geothermal powered subcritical and supercritical ORC are formed and the performances of these cycles are compared using these models. These models include a detailed thermal model of shell and tube heat exchanger integrating geothermal and ORC sides and basic thermodynamic models for the other components of the cycle. In the modeling of the heat exchanger, this device was divided into several zones and the outlet conditions of each zones were found applying energy balance and the LMTD method. This zone-modeling approach was also compared with the single-zone approach. The effect of

the source temperature on the performance and design of the heat exchanger was assessed for the subcritical and supercritical ORC. The following main conclusions were derived from this study.

- When the inlet and exit conditions of the ORC working fluid are considered as known, as the source temperature increases, the heat transfer surface area, the pressure drop, the exergetic efficiency, and the effectiveness of the heat exchanger decrease for subcritical and supercritical ORC.
- When multi-zone modeling approach is used instead of single-zone approach, at 430 K, the heat transfer surface area and the pressure drop increase by 57.56% and 68.26% for subcritical ORC, respectively; whereas they increase by 2.09% and decrease by 48.38% for supercritical ORC, respectively.
- The exergetic and electrical efficiencies of supercritical ORC are higher than those of the subcritical ORC.
- When the supercritical ORC is used, it was found that, more than 44.12% of net power is produced.
- The multi zone modeling approach is considered to give more accurate results than the single zone modeling approach.

Acknowledgment

The authors would like to thank to Dr. M. Akif Ezan and Mr. Gokhan Fidan for their help and guidance in the modelling of the heat exchanger. The authors also acknowlegde the contributions of Mrs. Duygu Melek Cakici in the modeling of the organic Rankine cycle.

Nomenclature

A – heat transfer surface area, [m^2]
D – diameter, [m]
$\dot{E}$ – exergy, [kW]
f_s – supercritical pressure friction factor
f_{tp} – two phase pressure friction factor
F – LMTD correction factor
g – gravity of acceleration, [ms^{-2}]
h – enthalpy, [kJ kg^{-1}]
h_i, h_c – convection heat transfer coefficient [Wm^{-2}K^{-1})
k – thermal conductivity, [Wm^{-1}K^{-1}]
L – length, [m]
$\dot{m}$ – mass flow rate, [kg s^{-1}]
n_{pass} – number of passes
N_t – number of tubes
Nu – Nusselt number
$\dot{Q}$ – heat transfer rate, [W]
R''_f – fouling factor, [m^{2}KW^{-1}]
Re – Reynolds number
s – entropy, [kJkg^{-1}K^{-1}]
T – temperature, [K]
U – overall heat transfer coefficient, [Wm^{-2}K^{-1}]
V – velocity, [ms^{-1}]
$\dot{W}$ – power, [kW]
x – quality
z – elevation, [m]

Greek symbols

ε – effectiveness
η – efficiency
ρ – density, [kgm^{-3}]
υ – specific volume, [m^{3}kg^{-1}]

Subscripts

c – cold
e – exit
el – electric
ex – exergy
f – fluid
g – gas
h – hot
hx – heat exchanger
i – inner, inlet, tube
net – net
o – outer, outlet, dead state, shell
wf – working fluid
zone – zone

References

[1] DiPippo, R., Geothermal Energy Electricity Generation and Environmental Impact, *Energy Policy*, *19*, (1991), 8, pp. 798-807
[2] Cakici, D. M., *et al.*, Thermodynamic Performance Assessment of an Integrated Geothermal Powered Supercritical Regenerative Organic Rankine Cycle and Parabolic trough Solar Collectors, *Energy*, *120* (2017), Feb., pp. 306-319
[3] Kanoglu, M., Exergy Analysis of a Dual-Level Binary Geothermal Power Plant, *Geothermics*, *31* (2002), 6, pp. 709-724
[4] DiPippo, R. Ideal Thermal Efficiency for Geothermal Binary Plants, *Geothermics*, *36* (2007), 3, pp. 276-285
[5] Phair, K. A., Getting the Most Out of Geothermal Power, *Mechanical Engineering*, 116 (1994), 9, pp. 76
[6] Kanoglu, M., Bolatturk, A., Performance and Parametric Investigation of a Binary Geothermal Power Plant by Exergy, *Renewable Energy*, *33* (2008), 11, pp. 2366-2374
[7] Erdogan, A., *et al*., Thermodynamic Optimisation of a Hybrid Solar-Geothermal Power Plant Using Taguchi Method, *International Journal of Exergy*, *23* (2017), 1, pp. 63-84
[8] DiPippo R., *Geothermal Power Plants: Principles, Applications, Case Studies and Environmental Impact*, Butterworth-Heinemann, UK, 2012
[9] Moro, R., *et al.*, ORC Technology for Waste-Wood to Energy Conversion in the Furniture Manufacturing Industry, *Thermal Science, 12* (2008), 4, pp. 61-73
[10] Kaya, A., *et al*., Design Sensitivity Analysis of a Plate-Finned Air-Cooled Condenser for Low-Temperature Organic Rankine Cycles, *Heat Transfer Engineering*, *38* (2017), 11-12, pp. 1018-1033
[11] Heberle, F., Bruggemann, D., Exergy Based Fluid Selection for a Geothermal Organic Rankine Cycle for Combined Heat and Power Generation, *Applied Thermal Engineering*, *30* (2010), 11, pp. 1326-1332
[12] Tempesti, D., Fiaschi, D., Thermo-Economic Assessment of a Micro CHP System Fuelled by Geothermal and Solar Energy, *Energy*, *58* (2013), Sept., pp. 45-51
[13] Wang, Z. Q., *et al*., Fluid Selection and Parametric Optimization of Organic Rankine Cycle Using Low Temperature Waste Heat, *Energy*, *4* (2012), 1, pp. 107-115
[14] Marion, M., *et al*., Study and Optimization of a Solar Subcritical Organic Rankine cycle, *Renewable Energy*, *48* (2012), Dec., pp. 100-109
[15] Kosmadakis, G., *et al*., Experimental Testing of a Low-Temperature Organic Rankine Cycle (ORC) Engine Coupled with Concentrating PV/Thermal Collectors, Laboratory and Field Tests, *Energy*, *117*, (2016), Part 1, pp. 222-236
[16] Barbazza L, *et al*., Optimal Design of Compact Organic Rankine Cycle Units for Domestic Solar Applications, *Thermal Science*, *18* (2014), 3, pp. 811-822
[17] ***, Turkiye'de Termik Santraller, TMMOB, Ankara, 2017
[18] Wang, E., *et al*., A Regenerative Supercritical-Subcritical Dual-Loop Organic Rankine Cycle System for Energy Recovery from the Waste Heat of Internal Combustion Engines, *Applied Energy*, *190* (2017), Mar., pp. 574-590
[19] Dong, B., *et al*., Analysis of the Supercritical Organic Rankine Cycle and the Radial Turbine Design for High Temperature Applications, *Applied Thermal Engineering*, *123* (2017), Aug., pp. 1523-1530
[20] Hsieh, J. C., *et al*., Design and Preliminary Results of a 20-kW Transcritical Organic Rankine Cycle with a Screw Expander for Low-Grade Waste Heat Recovery, *Applied Thermal Engineering*, *110* (2017), Jan., pp. 1120-1127
[21] Shengjun, Z., *et al*., Performance Comparison and Parametric Optimization of Subcritical Organic Rankine Cycle (ORC) and Transcritical Power Cycle System for Low-Temperature Geothermal Power Generation, *Applied Energy*, *88* (2011), 8, pp. 2740-2754
[22] Vetter, C., *et al*., Comparison of Sub and Supercritical Organic Rankine Cycles for Power Generation from Low-Temperature/Low- Enthalpy Geothermal Wells, Considering Specific Net Power Output and Efficiency, *Applied Thermal Engineering*, *5* (2013), 1, pp. 871-879
[23] Lazova, M., *et al*., Supercritical Heat Transfer and Heat Exchanger Design for Organic Rankine Applications, *Proceedings,* 11th International Conference on Heat Transfer, Fluid Mechanics, Thermodynamics Proceedings 2015, pp. 588-593
[24] Kakac, S., *et al*., A. *Heat Exchangers: Selection, Rating, and Thermal Design*, CRC Press, Boca Raton, Fla., Usa, 2012

[25] Calli, O., Performance Assessment of a Biomass Fired Regenerative ORC System through Energy and Exergy Analyses, in: *Exergetic, Energetic, Environmental Dimensions* (Eds. I. Dincer, C. O. Colpan, O. Kizilkan), Elsevier, New York, USA, 2017, pp. 253-277
[26] Erdogan, A., *et al*., Thermal Design and Analysis of a Shell and Tube Heat Exchanger Integrating a Geothermal Based Organic Rankine Cycle and Parabolic trough Solar Collectors, *Renewable Energy*, *109* (2017), Aug., pp. 372-391
[27] Zhang, C., *et al*., Thermo-Economic Comparison of Subcritical Organic Rankine Cycle Based on Different Heat Exchanger Configurations, *Energy*, *123* (2017), Mar., pp. 728-741
[28] Lazova, M., *et al*., Performance Evaluation of a Helical Coil Heat Exchanger Working under Supercritical Conditions in a Solar Organic Rankine Cycle Installation, *Energies*, *9* (2016), 6, pp. 1-20
[29] Harrison, J., (eds.) *Standards of the Tubular Exchangers Manufacturers Association*, 8th ed., Tubuluar Exchanger Manufactures Association, New York, USA, 2007
[30] Incropera, F. P., *et al*., *Fundamentals of Heat and Mass Transfer,* 7th ed*.,* John Wiley and Sons, New York, USA, 2012
[31] Kandlikar, S. G., A General Correlation for Saturated Two-Phase Flow Boiling Heat Transfer Inside Horizontal and Vertical Tubes, *ASME J. Heat Transfer*, *112* (1990), 1, pp. 219-228
[32] Fang, X., *et al*., Pressure Drop and Friction Factor Correlations of Supercritical Flow, *Nuclear Engineering and Design*, *242* (2012), Jan., pp. 323-330
[33] Ishihara, K., *et al*., Critical Review of Correlations for Predicting Two-Phase Flow Pressure Drop Across Tube Banks, *Heat Transfer Engineering*, *1* (1980), 3, pp. 23-32

Paper submitted: November 1, 2017
Paper revised: December 6, 2017
Paper accepted: December 11, 2017

© 2018 Society of Thermal Engineers of Serbia
Published by the Vinča Institute of Nuclear Sciences, Belgrade, Serbia.
This is an open access article distributed under the CC BY-NC-ND 4.0 terms and conditions